Noname manuscript No.
(will be inserted by the editor)

Superconductivity over 30 K of Nd_2CuO_4 films on CaF_2 substrates

Yoshiko Nanao · Michio Naito

Received: date / Accepted: date

Abstract Nd_2CuO_4 has a crystal structure called the Nd_2CuO_4 (T') structure in which fluorite-like Nd_2O_2 slabs and CuO_2 planes stack alternately. Nd_2CuO_4 is known to show superconductivity by carrier doping via anion/cation substitution, or making the oxygen sublattice highly ordered via a stringent control of thermodynamic conditions during crystal growth. In this study, CaF_2 is used for growing Nd_2CuO_4 films, as a substrate material which contains fluorine atoms. The films show superconducting onset (T_c^{on}) beyond 30 K. Furthermore, in contrast to reported superconductivity in this system, the emergence of superconductivity is found to be insensitive to post annealing procedures.

Keywords Cuprates · T' structure · superconductivity

PACS 74.10.+v · 74.25.Fy · 74.72.-h · 74.78.-w · 81.10.-h

Mathematics Subject Classification (2010) 82D55 · 74K35

Yoshiko Nanao
School of Physics and Astronomy
University of St. Andrews
JF Allen Building
North Haugh, St. Andrews, Fife, KY16 9SS
Scotland
E-mail: y05hik0nana0@gmail.com

Michio Naito
Department of Applied Physics
Tokyo University of Agriculture and Technology
2–24–16, Naka-cho, Koganei, Tokyo 184-8588
Japan

1 Introduction

The first discovery of superconductivity in copper oxide [1] drove researchers into intensive competitions to find new superconductors with higher superconducting transition temperature (T_c), and to clarify the origin of high temperature superconductivity in copper oxide system. Many materials found to show superconductivity by hole doping, while there are relatively fewer examples of electron-doped superconductors; one example is the infinite layer (IL) materials [2–4], and another is RE_2CuO_4 (RE: rare earth elements) with the Nd_2CuO_4 (T') structure (Figure 1 (a)). In both IL structure and T' structure, copper atoms are square-planar coordinated by surrounding oxygen atoms, and form CuO_2 planes. The CuO_2 planes are sandwiched by alkali earth ions in IL structure, and by fluorite-like RE_2O_2 blocks in the T' structure, respectively.

In the system of T'-RE_2CuO_4, superconductivity can be induced by substituting either RE atoms or oxygen atoms. First superconductivity was reported in cerium doped $(Nd,Ce)_2CuO_4$ [5], followed by thorium doped $RE_{2-x}Th_xCuO_4$ (RE = Pr [6], Nd [7], Sm [8]) and fluorine doped $Nd_2Cu(O,F)_4$ [9]. In the references above, bulk (powder) samples were examined and the emergence of superconductivity are explained on the basis of carrier doping into insulating parent materials. On the other hand, thin films of non-dope compounds are fairly metallic after post annealing process in vacuum. It has been known empirically that apical oxygen atoms above copper atoms in T' copper oxides play the role of a very strong scatterer as well as a pair breaker. Obtaining a perfect oxygen sublattice (i.e., fully filled in-plane oxygen sites without residual apical oxygen atoms) requires a precise control of oxidisation/reduction conditions. 20 years after the first report

[5], thin films of RE_2CuO_4 (RE = Pr, Nd, Sm, Eu, Gd), synthesised by means of metal-organic decomposition, was found to show superconductivity with substantially higher T_c compared to those of electron-doped relatives [10]. For example, non-dope Nd_2CuO_4 films show superconductivity onset as high as $T_c^{on} \sim 33$ K, in contrast to $T_c^{on} \sim 24$ K in $(Nd,Ce)_2CuO_4$ [5], and ~ 27 K in $Nd_2Cu(O,F)_4$ [9]. This implies that thin film samples are advantageous in removal of the apical oxygen atoms due to a large surface-to-volume ratio. Another advantage of film samples is the use of substrate materials which provides lattice strains as well carrier doping driven by atomic diffusion from the substrate/film interface.

In this work, we synthesised film samples of Nd_2CuO_4 on (001) CaF_2 substrates in order to revisit the results on superconducting $Nd_2Cu(O,F)_4$ [9,11]. Nd_2CuO_4 films on (001) CaF_2 show sharp superconducting transition at higher temperature compared to previously reported $Nd_2Cu(O,F)_4$. The highest $T_c^{on} \sim 31$ K, which is almost as high as that of non-dope Nd_2CuO_4 films on oxide substrates [10]. Furthermore, the metallic conduction and superconductivity in the films of Nd_2CuO_4 on (001) CaF_2 was found to be independent of post annealing process in contrast to what is reported for superconducting non-dope Nd_2CuO_4 films on oxide substrates such as $SrTiO_3$ and $DyScO_3$.

2 Experimental

Controlling both stoichiometry and thermodynamic conditions is a key to synthesise single phase crystals, particularly those of complex oxide of transition metals. Molecular beam epitaxy (MBE) is a synthesis technique which enables simultaneous and precise manipulation of both stoichiometry and thermodynamic conditions, and therefore, is known to produce the unparalleled crystal quality. All the films in this study were synthesised in a custom-made MBE chamber which is kept at base pressure $\sim 10^{-6}$ Pa (figure 1 (b)). For stabilising the desired phase, atomic oxygen is supplied as an oxidant using RF oxygen plasma source. The power of plasma source and O_2 gas flow into the plasma source are varied in the range of 250 W to 350 W, and 0.8 sccm to 1.2 sccm, respectively. The equilibrium pressure during film deposition is typically $\sim 1.5 \times 10^{-3}$ Pa to 3.0×10^{-3} Pa. The atomic fluxes from metal sources (Nd and Cu) are calibrated against quartz crystal microbalance (QCM). Electron impact emission spectroscopy (EIES) and feedback loop are used for monitoring and controlling the atomic fluxes and stoichiometry. The atomic fluxes of constituent elements are adjusted to give the growth rate ~ 0.1 unit-cell layer/second. The film thickness is typically ~ 800 Å. The deviations from optimal growth conditions, e.g., off-stoichiometry of cation ratio, often result in precipitation of unwanted phases and degradation of in-plane coherency of the crystal. Reflection high energy electron diffraction (RHEED) is used to monitor the surface morphology during the film growth and to detect such signals of deterioration of crystalline quality. Fluorine doping is attempted by using (001) CaF_2 substrates assuming diffusion of fluorine atoms from the substrate into the film. For the deposition, substrate temperature $T_s \sim 730$ °C was used for all the samples. In the case of non-dope Nd_2CuO_4 films grown on oxide substrates, post annealing process is essential otherwise superconductivity is destroyed by electron scattering by residual apical oxygen atoms. Therefore, some films were kept at ~ 580 °C in vacuum for 10 minutes after the deposition. Films which are not annealed are denoted as as-grown films. X-ray diffraction (XRD) is used in order to identify the grown phases, to evaluate the crystalline quality, as well as to determine the c-axis lattice constant (c_0). Standard four-probe method is used for resistivity measurements.

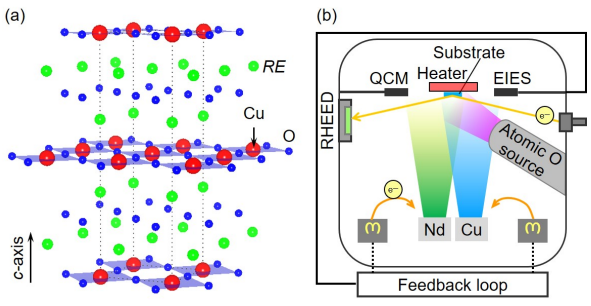

Fig. 1 (a)(left) The Nd_2CuO_4 structure (also called T' structure). Trivalent rare earth ions (e.g., La^{3+}, Pr^{3+}, Sm^{3+}, Eu^{3+}, Gd^{3+}, Tb^{3+}), as well as tetravalent ions (Ce^{4+}, Th^{4+}) can be located in the RE sites. Similarly, the oxygen sites can be altered by halogen elements (e.g., F^-). (b)(right) A schematic of MBE chamber used in this study.

3 Results

From X-ray diffraction patterns, it was confirmed that c-orientated Nd_2CuO_4 films are synthesised over the examined range of growth parameters. All films show positive temperature derivative of resistivity ($\frac{d\rho}{dT}>0$) from 300 K to ~ 70 K. Non-superconducting films show upturn in lower temperature range likely due to lattice defects. The resistivity curves of superconducting Nd_2CuO_4 films on CaF_2 are shown in figure 2. The typical resistivity values at 300 K ranged 400 $\mu\Omega$cm to 800 $\mu\Omega$cm, and sharp superconducting onsets are observed at $T_c^{on} \sim 30$ K. Comparing with the resistivity

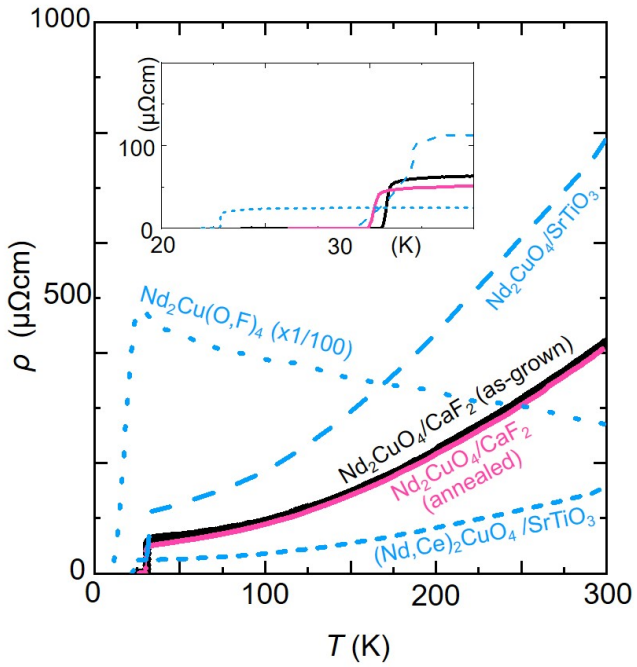

Fig. 2 Temperature dependences of electrical resistivity (ρ-T) in the Nd_2CuO_4 films grown on (001) CaF_2 substrates synthesised in this work. The black and pink curves correspond to as-grown film and annealed film, respectively. For a comparison, ρ-T curves of Nd_2CuO_4 film on $SrTiO_3$ [12] (dashed line), $(Nd,Ce)_2CuO_4$ film on $SrTiO_3$ [13] (short dashed line), and $Nd_2Cu(O,F)_4$ pellet [9] (dotted line, multiplied by $\frac{1}{100}$) are also shown. The inset shows an enlarged view between 20 K to 35 K. The film samples in this work show lower resistivity values and higher T_c values compared to those reported for $Nd_2Cu(O,F)_4$ pellet regardless of post annealing process.

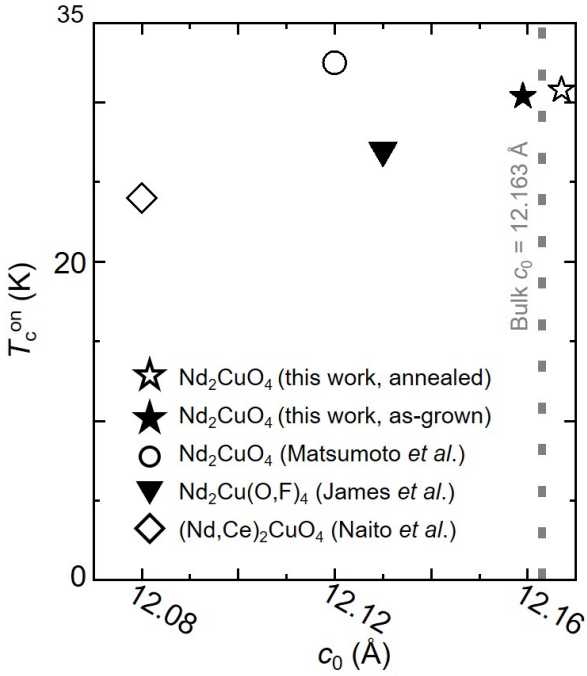

Fig. 3 Temperatures of superconducting onset (T_c^{on}) as a function of c-axis lattice constant (c_0) for films in this study (plotted with stars), non-dope superconducting Nd_2CuO_4 film [10] (circle), optimally doped $(Nd,Ce)_2CuO_4$ film [13] (diamond), and $Nd_2Cu(O,F)_4$ pellet [9] (downward triangle). Filled marks correspond to as-grown samples [14]. For a comparison, the c_0 value in bulk Nd_2CuO_4 [15] is also shown as dotted grey line. The Nd_2CuO_4 films grown on (001) CaF_2 substrates have comparable c_0 with the bulk value, and it is almost independent of post annealing process.

curve reported for the bulk $Nd_2Cu(O,F)_4$ in [9] (figure 2, dotted line), much lower resistivity values as well as higher superconducting transition temperature are observed in this study. Moreover, the emergence of superconductivity and the values of T_c^{on} in this study seems independent of annealing process, in contrast to cases of cerium doped and non-dope Nd_2CuO_4 films in which post annealing in vacuum is critical to superconducting properties.

The insensitive response to annealing process can be seen in not only electrical conduction but also structural parameters. Figure 3 illustrates T_c^{on} as a function of c_0 for samples shown in figure 2. Figure 3 also include data from [9, 12, 13]. Here, the c-axis lattice constants of films are estimated by applying Nelson-Relay function to the d values of diffraction peaks from Nd_2CuO_4 [16]. Filled marks correspond to as-grown samples. For a comparison, the c_0 value in bulk Nd_2CuO_4 [15] is also shown as dotted grey line. The Nd_2CuO_4 films grown on (001) CaF_2 substrates (shown as stars) have c_0 close to the bulk value, and the T_c^{on}s do not change depending on c_0 values. On the other hand, substantially shorter value is reported for fluorine doped $Nd_2Cu(O,F)_4$ powder samples (12.13 ± 0.02 Å) [9] (triangle) and for cerium doped $(Nd,Ce)_2CuO_4$ (12.08 Å) [13] (diamond) due to replacement with ions with smaller ionic radii (i.e., O^{2-}: 1.40 Å $\rightarrow$ F^-: 1.33 Å, and Nd^{3+}: 1.109 Å $\rightarrow$ Ce^{4+}: 0.97 Å [17]). Without ion substitution, the superconducting films of non-dope Nd_2CuO_4 on oxide substrates, in which eliminating apical oxygen atoms is crucial to superconductivity, also show shorter c_0 value compared to the bulk value. In the case of non-dope Nd_2CuO_4 on oxide substrates, c_0 changes depending on the residual amount of apical oxygen atoms [18]. Therefore, c_0 qualitatively indicate the residual amount of apical oxygen atoms. For example, the typical c_0 value of non-dope superconducting Nd_2CuO_4 films on oxide substrates is considerably (~ 0.03 Å to 0.04 Å) shorter than bulk c_0 [10].

The original intention to employ fluorite substrates was to dope fluorine atoms as donors via atomic diffusion. Some of Nd_2CuO_4 films grown on (001) CaF_2

indeed show superconductivity However, the results appear not to be explained by simple fluorine doping because the observed values of T_c^{on} are substantially higher and the c_0s are longer compared to the reported values for bulk (powder) $Nd_2Cu(O,F)_4$ [9].

There are some scenarios to possibly explain the result. One is that the observed superconductivity stems from non-dope Nd_2CuO_4 domains in the samples. As reported in [19], with the growth condition marginal for the T' phase formation, i.e., by increasing growth temperature and reducing oxygen partial pressure from typical growth condition, non-dope T' materials show superconductivity in the as-grown state. It is known that oxide substrates supply additional oxygen atoms which increase the oxygen partial pressure in the surface selectively. On the other hand, no oxygen diffusion occur from fluorite substrates, which may result in similar growth condition as described in [19]. However, the observed insensitivity to post annealing process and the peculiarly long c_0 for its high its high T_c^{on} may be contradictory to the preceding reports on superconductivity in the non-dope system on oxide substrates.

Another is that the superconductivity is induced by fluoridation of $Nd_2CuO_{3.5}$. Corbel *et al.* [20] suggested that, through fluoridation at 200 °C to 300 °C, fluorine atoms replace oxygen atoms in the Nd_2O_2 slab and the released oxygen atoms migrate in to the $CuO_{1.5}$ layers thus forming conducting CuO_2 planes. This anion rearrangement induces structural deformation from monoclinic symmetry to tetragonal symmetry. Similar structural deformations are previously found in fluoridation or oxidisation of A_2CuO_3 (A = Ca, Sr, Ba) [21–25]. Fluoridated $Nd_2CuO_{3.5}$ show superconductivity at $T_c^{on} \sim 6$ K to 11 K, which is lower than the maximal $T_c^{on} \sim 27$ K in $Nd_2Cu(O,F)_4$. Not optimal Cu oxidation state and a partial substitution of in-plane oxygen sites by fluorine atoms are attributed as possible reasons in [20], yet the exact reason for lowering T_c in fluoridated $Nd_2CuO_{3.5}$ remains unclear. It is reported that a majority of fluorine atoms substitute for the oxygen sites in Nd_2O_2 blocks, while approximately 30 % of fluorine atoms also substitute in in-plane oxygen sites [20,26,27]. Calculation of the electrostatic energies for different oxygen and fluorine distributions between the Nd_2O_2 blocks (i.e., $Nd_2(O,F)_2{\cdot}CuO_2$) and CuO_2 (i.e., $Nd_2O_2{\cdot}Cu(O,F)_2$) planes was performed by [20]. The calculation showed that the former structure has a lower energy than the latter by ~ 200 kJ/mol. Due to the non-equillibrium character of MBE growth, occupation or migration of fluorine atoms to in-plane sites might be suppressed in this study, which results in improved electronic conduction. It must be noted, however, that the c_0 values of Nd_2CuO_4 films on CaF_2 close to the bulk c_0 seem contradictory to crystallographic consideration: c_0 values are expected to be reduced by substituting oxygen atoms by smaller fluorine atoms. Perhaps, part of the doped fluorine atoms may occupy the apical sites which may provide additional hole to CuO_2 planes from the viewpoint of valence state of copper ions. However, it is uncommon that fluorine atoms occupy the apical sites while the crystal lattice keeps the T' structure [28].

Indeed, there are only few reports on "hole-doped" superconductors with T' structure. Takamatsu *et al.* reported superconductivity in $La_{1.8-x}Eu_{0.2}A_xCuO_4$ (A = Ca, Sr) [29,30]. In both composition, the materials stabilise in T' structure, and both show $T_c^{on} \sim 13$ K with $x = 0.05$. In [29,30], the examined powder samples had a few % of superconducting volume fractions which may be attributed to oxygen sublattice disorder, i.e., in-plane oxygen defect and/or residual apical oxygen atoms. However, this difficulty can be overcome in films samples due to a large surface-to-volume ratio [10]. Note that, however, superconductivity in this system strongly depends on the synthesis process, and therefore hole-doped superconductivity in T' copper oxides is not a consensus yet that [31].

4 Conclusion

Film synthesis of Nd_2CuO_4 using CaF_2 substrate was attempted. The films grown were confirmed to be Nd_2CuO_4 with T' structure from X-ray diffraction pattern. Some films show sharp superconducting transition and $T_c^{on} \sim 31$ K at highest. In contrast to previously reported trends in neighbouring systems, the values of T_c^{on} and c-axis lattice constant appeared independent of post annealing process. Further characterisations are required to clarify the origin of superconducting phase observed in this study.

References

1. J.G. Bednorz, K.A. Müller, Zeitschrift für Physik B Condensed Matter **64**(2), 189 (1986)
2. M. Takano, M. Azuma, Z. Hiroi, Y. Bando, Y. Takeda, Physica C: Superconductivity **176**(4-6), 441 (1991)
3. M. Smith, A. Manthiram, J. Zhou, J. Goodenough, J. Markert, Nature **351**(6327), 549 (1991)
4. G. Er, Y. Miyamoto, F. Kanamaru, S. Kikkawa, Physica C: Superconductivity **181**(1-3), 206 (1991)
5. H. Takagi, S. Uchida, Y. Tokura, Physical review letters **62**(10), 1197 (1989)
6. J. Markert, E. Early, T. Bjørnholm, S. Ghamaty, B. Lee, J. Neumeier, R. Price, C. Seaman, M. Maple, Physica C: Superconductivity **158**(1-2), 178 (1989)
7. J. Markert, M. Maple, Solid state communications **70**(2), 145 (1989)

8. E. Early, N. Ayoub, J. Beille, J. Markert, M. Maple, Physica C: Superconductivity **160**(3-4), 320 (1989)
9. A. James, D. Murphy, S. Zahurak, Nature **338**(6212), 240 (1989)
10. O. Matsumoto, A. Utsuki, A. Tsukada, H. Yamamoto, T. Manabe, M. Naito, Physical Review B **79**(10), 100508 (2009)
11. H. Koinuma, K. Takeuchi, M. Yoshimoto, K. Hashida, M. Nakabayashi, S. Gonda, T. Hirayama, T. Shiraishi, Japanese Journal of Applied Physics **29**(9A), L1642 (1990)
12. O. Matsumoto, A. Tsukada, H. Yamamoto, T. Manabe, M. Naito, Physica C: Superconductivity and its applications **470**(20), 1029 (2010)
13. M. Naito, H. Sato, H. Yamamoto, Physica C: Superconductivity **293**(1-4), 36 (1997)
14. The polycrystalline superconducting $Nd_2Cu(O,F)_4$ samples were obtained only after annealing at 890 °C in flowing nitrogen gas. The effect of this nitrogen annealing is explained as to result in a greater degree of fluorine substitution.
15. T. Uzumaki, K. Hashimoto, N. Kamehara, Physica C: Superconductivity **202**(1-2), 175 (1992)
16. J.B. Nelson, D. Riley, Proceedings of the Physical Society **57**(3), 160 (1945)
17. R.D. Shannon, Acta crystallographica section A: crystal physics, diffraction, theoretical and general crystallography **32**(5), 751 (1976)
18. The *c*-axis lattice constants can be shortened by annealing in reductive environment in $(RE,Ce)_2CuO_4$
19. Y. Krockenberger, M. Horio, H. Irie, A. Fujimori, H. Yamamoto, Applied Physics Express **8**(5), 053101 (2015)
20. G. Corbel, J. Attfield, J. Hadermann, A. Abakumov, A. Alekseeva, M. Rozova, E. Antipov, Chemistry of materials **15**(1), 189 (2003)
21. M. Al-Mamouri, P.P. Edwards, C. Greaves, P.R. Slater, M. Slaski, Journal of Materials Chemistry **5**(6), 913 (1995)
22. M. Ai-Mamouri, P. Edwards, C. Greaves, M. Slaski, Nature **369**(6479), 382 (1994)
23. S.i. Karimoto, H. Yamamoto, T. Greibe, M. Naito, Japanese Journal of Applied Physics **40**(2B), L127 (2001)
24. H. Yamamoto, M. Naito, H. Sato, Japanese Journal of Applied Physics **36**(3B), L341 (1997)
25. W. Gao, Q. Liu, L. Yang, Y. Yu, F. Li, C. Jin, S. Uchida, Physical Review B **80**(9), 094523 (2009)
26. J.H. Kim, C.E. Lee, Physical Review B **53**(5), 2265 (1996)
27. A. Krol, Y. Soo, Z. Ming, S. Huang, Y. Kao, G. Smith, K. Lee, A. James, D. Murphy, Physical Review B **46**(1), 443 (1992)
28. J. Kissick, C. Greaves, P. Edwards, V. Cherkashenko, E. Kurmaev, S. Bartkowski, M. Neumann, Physical Review B **56**(5), 2831 (1997)
29. T. Takamatsu, M. Kato, T. Noji, Y. Koike, Applied Physics Express **5**(7), 073101 (2012)
30. T. Takamatsu, M. Kato, T. Noji, Y. Koike, Physics Procedia **58**, 46 (2014)
31. M. Fujita, K. Tsutsumi, T. Miura, S. Danilkin, in *Journal of Physics: Conference Series*, vol. 969 (IOP Publishing, 2018), vol. 969, p. 012070